Numerical complexity study of solving hybrid multiport field-circuit problems for diode grids

Numerical Complexity Study of Solving Hybrid Multiport Field-Circuit Problems for Diode Grids

Torben Wendt, Cheng Yang and Christian Schuster
Institute of Electromagnetic Theory
Hamburg University of Technology
Hamburg, Germany
torben.wendt, cheng.yang, schuster@tuhh.de

S. Grivet-Talocia
Dept. of Electronics and Telecommunications
Politecnico di Torino
Torino, Italy
stefano.grivet@polito.it

***Abstract*—Nonlinearly loaded multiport structures have promising features for the application of controlling scattered fields. Modelling such structures can lead to investigations up to hundreds or even thousands of ports, which poses a challenge to full-wave simulation techniques. In order to identify limitations for large scale problems, a hybrid simulation method using macromodeling and recursive convolution is adopted due to its scalability. A numerical complexity analysis is carried out for the extraction of frequency data, macromodeling of the network parameters and computation of transient responses. Of particular interest are the number of ports, load types, wave excitations and field probes. Bottlenecks are identified and possible improvements of the adopted method are proposed.**

***Index Terms*—Numerical complexity, multiport, field-circuit, diode grids**

I. Introduction

Resilience against High Intensity Radiated Fields (HIRF), caused by e.g. base stations or lightning strikes, is required for the reliability of communication devices. To protect a device from strong fields, electromagnetic shielding is applied by putting the device into a conducting enclosure with one or more apertures to allow for communication. However, the aperture also becomes the entry for incident HIRF which is a threat to the electronics. To shield the cavity from destructive energy levels, nonlinear elements can be used. In [1], [2] a grid of diodes forms an energy selective screen that covers the aperture of the cavity was investigated, as shown in Fig. 1. For weak incoming fields, the diodes experience induced voltages below the diodes threshold voltage and acts like an open grid and incident fields pass through the cover and enter the cavity. Once a certain energy level of the incoming field is surpassed, the induced voltages drive the diode screen to be conductive and acts as a shorted grid. It effectively closes the aperture for the incident field.

Similar nonlinear structures have a recently received attention in other applications, e.g. frequency selective surfaces [3], [4], waveform-dependent absorbing metasurfaces [5], [6], and power-dependent impedance surfaces [7], [8]. Systematic parameter studies of these structures require many numerical simulations and is time and memory consuming.

Available tools with full-wave field-circuit capabilities include the commercial, Finite Integration Technique (FIT) based software provided by [9], [10], Time Domain Integral Equation (TDIE) based solver developed by [11], Finite Element-Time Domain (FETD) based solver developed by [12], Method of Moments (MoM) base solver proposed by [13], [14]. From the perspective of numerical computation, the first three full-wave simulators working in time domain are universal but suffer from boundary truncation and computation inefficiency problems in case of frequently changing the configuration of wave excitation and port loads. In contrast, the last hybrid method are free of boundary truncation and could be very flexible for specified problems.

For studying the numerical complexity of nonlinearly loaded problems we employ a hybrid method that allows to simulate structures with many nonlinear loads [15]. Here we focus on the frequency data, the transient data analysis and discuss the computation and storage consumption for many ports, loads and observation points.

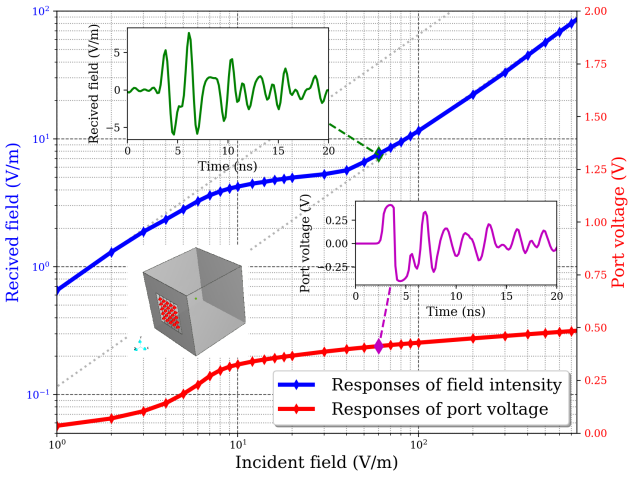

Fig. 1. Illustration of the field intensity dependent properties of a 5×5 (25 ports) diode grid, which is mounted across the aperture of the cavity depicted in the lower left. The ports of the structure are shown in red, each terminated with anti-parallel diodes.

This work is supported by the German Research Foundation.

II. Modelling Approach and Implementation

An electrically large structure loaded with lumped nonlinear elements is illuminated by a plane wave pulse with waveform $\mathcal{E}_{\text{inc}}(t)$. The target is to compute the electric field at an observer $\vec{\mathcal{E}}_{\text{obs}}(t)$, which depends nonlinearly on the incident pulse due to the nonlinear elements. We model the field coupling at the lumped ports using a Thevenin equivalent of the excited linear structure (see [16], [15]). Figure 2 shows the consecutive steps taken in order to construct the Thevenin equivalent and compute the voltages $v(t)$ across the nonlinear loads. First, the short circuit currents $i_{\text{sc}}(t)$ induced by $\mathcal{E}_{\text{inc}}(t)$ are computed as shown in Fig. 2a, which, together with the impedance parameter impulse response $\boldsymbol{\mathcal{z}}(t)$, are used to compute the open circuit voltage $v_{\text{oc}}(t)$. Second, cast the Thevenin equivalent of the excited structure using $\boldsymbol{\mathcal{z}}(t)$ and $v_{\text{oc}}(t)$ as shown in Fig. 2b. Third, attached the nonlinear loads to the ports as displayed in Fig. 2c and solve the network for the voltages across the nonlinear loads $v(t)$. Finally, by using the substitution theorem, replace the nonlinear loads with ideal voltage sources which enforcing v at the port and compute the scattered field $\vec{\mathcal{E}}_{\text{s}}(t)$ (Fig. 2d). Casting the hitherto described procedure into time domain equations for a single excitation and multiple ports and observers yields

$$\boldsymbol{v}_{\text{oc}}(t) = \boldsymbol{\mathcal{b}}(t) * \mathcal{E}_{\text{inc}}(t), \tag{1}$$

$$\boldsymbol{v}(t) = \begin{cases} \mathcal{F}(\boldsymbol{i}(t)), \\ \boldsymbol{v}_{\text{oc}}(t) - \boldsymbol{\mathcal{z}}(t) * \boldsymbol{i}(t), \end{cases} \tag{2}$$

$$\vec{\mathcal{E}}_{\text{obs}}(t) = \boldsymbol{c}(t) * \boldsymbol{v}(t) + \boldsymbol{\mathcal{d}}(t) * \mathcal{E}_{\text{inc}}(t), \tag{3}$$

where the linear impulse response describing the linear properties of the structure relate the following quantities: $\boldsymbol{\mathcal{b}}(t)$: excitation and induced, open circuit port voltage, $\boldsymbol{c}(t)$: port voltage and caused field at the observer; $\boldsymbol{\mathcal{d}}(t)$: excitation and field at the observer with short circuited ports. Finally, $\mathcal{F}$ is the nonlinear voltage-current relationship of the load, e.g. the Shockley diode equation.

The computation of the field at an observer is conducted in three consecutive stages as presented in Fig. 3. First, we adopt a frequency domain MoM solver [17] to compute the corresponding transfer functions of the impulse responses $\boldsymbol{\mathcal{b}}(t)$, $\boldsymbol{c}(t)$, $\boldsymbol{\mathcal{d}}(t)$ and $\boldsymbol{\mathcal{z}}(t)$, yielding the discrete frequency data $\breve{\mathbf{B}}(j\omega_n)$, $\breve{\mathbf{C}}(j\omega_n)$, $\breve{\mathbf{D}}(j\omega_n)$ and $\breve{\mathbf{Z}}(j\omega_n)$, respectively. Using vector fitting techniques, the respective rational function approximations $\mathbf{B}(s)$, $\mathbf{C}(s)$, $\mathbf{D}(s)$ and $\mathbf{Z}(s)$ are computed (passivity of network parameters is enforced). Second, eq. (1) is solved in discrete time version by evaluating $\mathbf{B}(j\omega_n)$ in time domain using recursive convolution (see [18]), yielding $v_{\text{oc}}(t_n)$. Together with an equivalent circuit synthesized from $\mathbf{Z}(s)$ and the $\mathcal{F}$, the nonlinear circuit shown in Fig. 2c is formulated as a SPICE netlist (see also eq. (2)) and solved using [19], yielding $v(t_n)$. Third, eq. (3) is solved in discrete time domain by interfacing $\mathbf{C}(s)$ and $\mathbf{D}(s)$ using recursive convolution, eventually yielding the desired $\vec{\mathcal{E}}_{\text{obs}}(t_n)$.

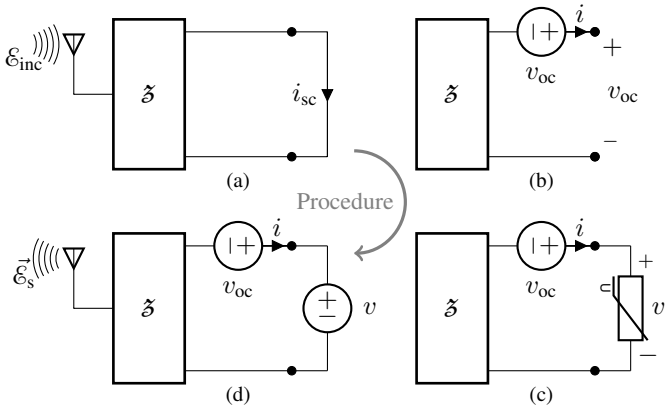

Fig. 2. Thevenin equivalent of the electromagnetic coupling.

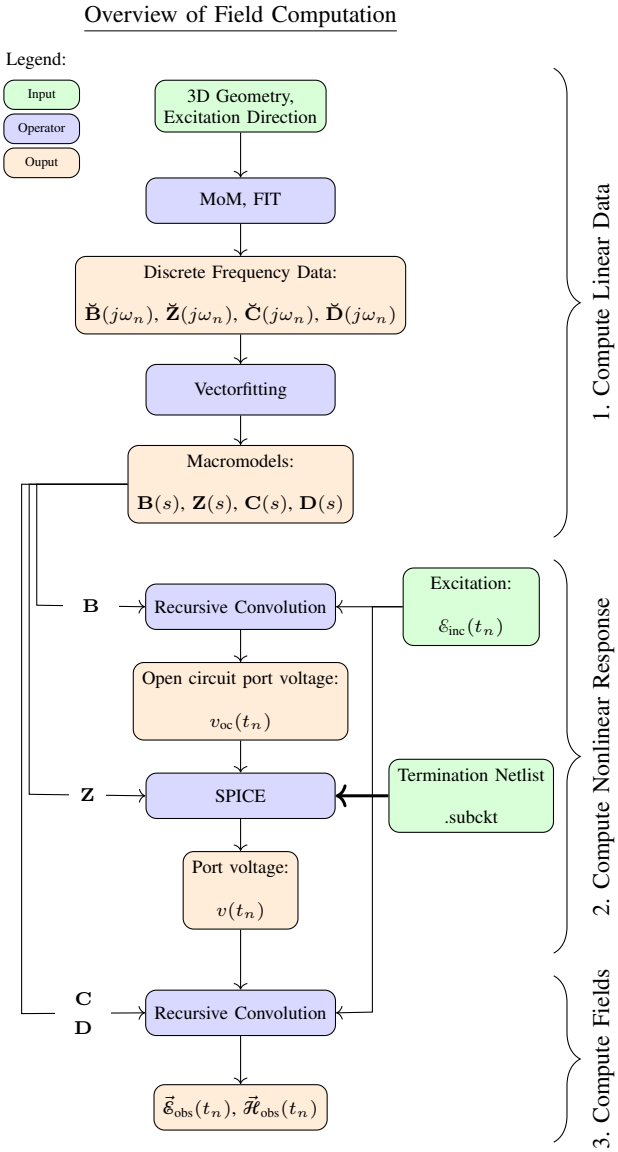

Fig. 3. General overview of the adopted hybrid field-circuit method.

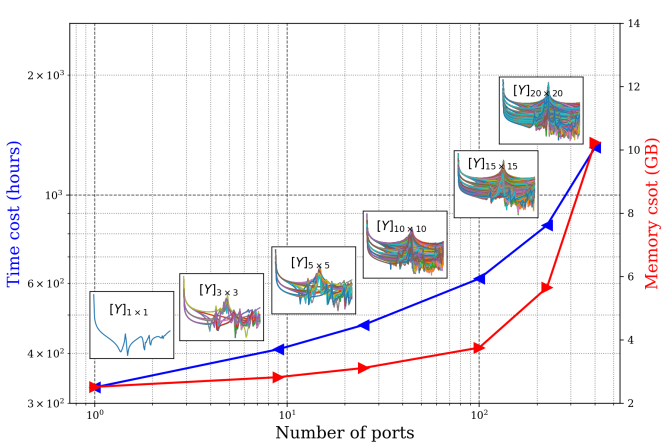

Fig. 4. Effort of the network parameters computation using MoM depending on the number of ports.

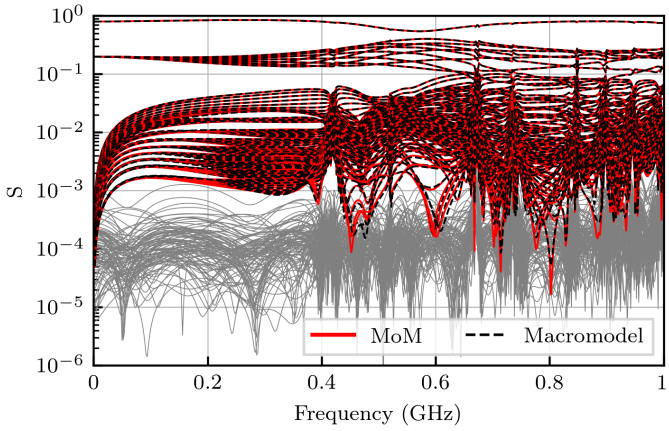

Fig. 5. Comparison of the the orignal frequency data obtained from MoM for the cavity with a 10×10 diode grid and the extracted macromodel with passivity enforcement. The grey curves show the fitting error for each element of the network parameters in frequency domain.

TABLE I
COMPUTATIONAL EFFORT FOR STRUCTURES WITH DIFFERENT NUMBERS OF PORTS USING MOM.

Structure	Unknowns	Patches	Size of System Matrix (MB)
Box1	5475	3704	457
Box9	6039	4152	556
Box25	6372	4442	619
Box100	6774	4792	700
Box225	7621	5620	886
Box400	8872	6818	1201

III. STUDY OF NUMERICAL COMPLEXITY

The computational and memory cost depend strongly on the number of excitations K, the number of ports P and the number of observers O. This section gives estimates of the required resources depending on these parameters and identifies bottlenecks and limitations. The complexity of computing the discrete frequency data (step one of Fig. 3) depends on P as shown in Fig. 4, because adding ports often leads to a finer mesh in the vicinity of the ports, increasing the number of patches and thus the number of unknowns as shown in Table I. The memory required to store one frequency point is derived from the dimensions of the tensors $\breve{\mathbf{B}}(j\omega_n) \in \mathbb{C}^{\mathrm{K}\times\mathrm{P}}$, $\breve{\mathbf{C}}(j\omega_n) \in \mathbb{C}^{\mathrm{P}\times\mathrm{O}\times3}$, $\breve{\mathbf{D}}(j\omega_n) \in \mathbb{C}^{3\times\mathrm{O}\times\mathrm{K}}$ and $\breve{\mathbf{Z}}(j\omega_n) \in \mathbb{C}^{\mathrm{P}\times\mathrm{P}}$, where each field is a complex double and requires 16 Byte. yielding an estimation for the required memory per frequency sample

$$\mathrm{M_{est}} = (\mathrm{K}\cdot\mathrm{P} + \mathrm{P}\cdot\mathrm{O}\cdot3 + \mathrm{K}\cdot\mathrm{O}\cdot3 + \mathrm{P}\cdot\mathrm{P})\cdot 16\,\mathrm{Byte}. \quad (4)$$

Table II lists the memory cost for the different test cases for each transfer function tensor, as well as the total required memory per frequency sample. As the number of frequency samples are in the number of thousands, we expect the required memory to be in the tens of GB, which recommends the investigation of compression techniques. Extracting the network parameter macromodel $\mathbf{S}$ for the 10x10 grid yields excellent

TABLE II
ESTIMATED MEMORY COST PER FREQUENCY SAMPLE OF INVESTIGATED EXAMPLES FOR DIFFERENT CONFIGURATIONS.

Diode Grid	3x3	7x7	10x10
Excitations (K)	4	4	20
Ports (P)	49	100	400
Observers (O)	8	20	500
$\mathbf{B}$ (kB)	3.136	6.4	128.
$\mathbf{C}$ (kB)	18.816	96.	9600.
$\mathbf{D}$ (kB)	1.536	3.84	480.
$\mathbf{Z}$ (kB)	38.416	160.	2560.
$\mathrm{M_{est}}$ (MB)	0.061904	0.26624	12.768

agreement as demonstrated in Fig. 5, but is time consuming. Once extracted, we successfully enforce the passivity of the model, which requires multiple hours on a consumer laptop. The extraction of the scalar macromodels collected in the tensors $\mathbf{B}(s)$, $\mathbf{C}(s)$, $\mathbf{D}(s)$ and $\mathbf{Z}(s)$ is easily parallelized, because all transfer functions are decoupled. Contrary to the network parameters, no passivity enforcement is necessary and the accuracy requirements are lower, as the models are only evaluated in one direction. However, for many excitations or ports or observers the number of scalar transfer functions grows quickly as demonstrated in Table II, which again recommends the use of compression techniques in the future to exploit sparsity of the data. Once extracted from the previously computed frequency data, the macromodels can be interfaced in time domain by recursive convolution (see eq. (1) and (3)). To solve eq. (2) using [19], the network parameter macromodel is synthesized as a SPICE compatible netlist.

In the following, a set of exemplary configurations is presented, highlighting the versatility of the adopted method. Fig. 6a shows both port voltages and electric field at an observer for different diode grid scales, exhibiting different responses to a gaussian pulse incident perpendicularly to the

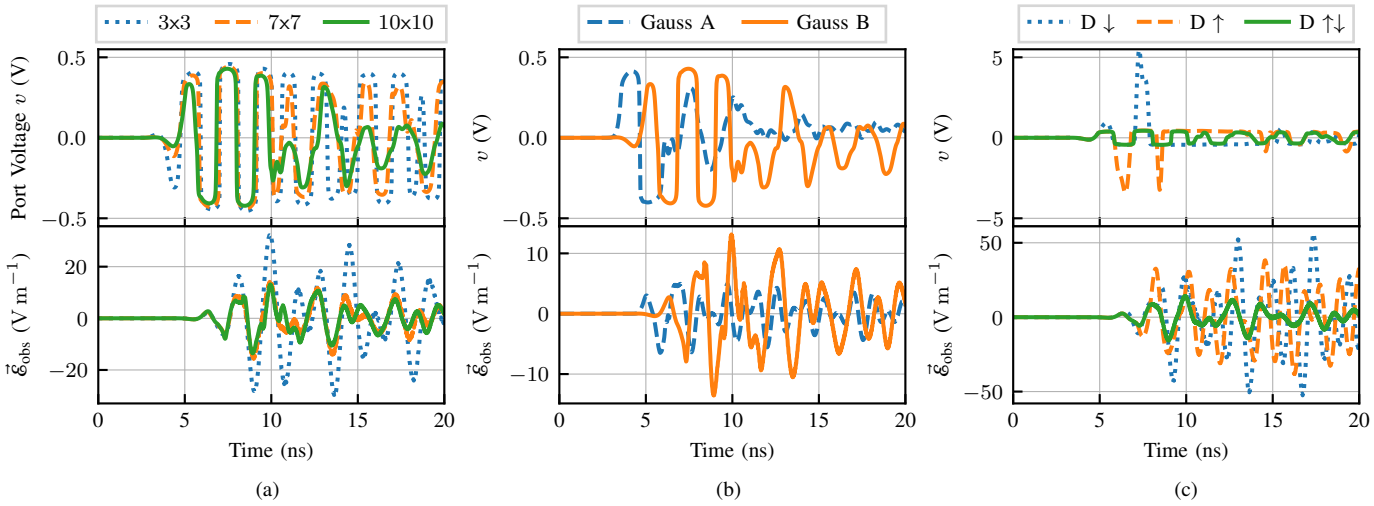

Fig. 6. Comparison of transient responses of the investigated cavity for (a) different scales of the diode grid, (b) different excitations (Gauss A: wide band and Gauss B: narrow band gaussian pulse) and (c) three different types of nonlinear loads (D ↑: single diode, D ↓: single diode opposite direction, D↑↓: antiparallel diodes).

grid with a peak value $150\,\mathrm{V\,m^{-1}}$. We observe that the 7x7 and 10x10 diode grid lead to similar attenuation of the received field compared to the 3x3 grid. Fig. 6b gives the transient responses of the 10x10 configuration for two excitation waveforms with different bandwidths. Fig. 6c demonstrates three diode configurations with different rectification behaviour lead to different amplitudes of the received field. Besides, in order to visualize the fields distribution, the number of observation points can easily be increased up to thousands by post-processing without having to repeat the full wave simulation.

IV. Conclusion

A hybrid field-circuit simulation method was employed to compute the scattered field of nonlinear diode grids. By comparing simulation cost for different configurations, the numerical complexity of the method was investigated with respect to scalability. Especially, the memory requirements depending on the number of excitations, the scale of the network and the amount of observation points were discussed in detail. Limitations were studied for up to hundreds of ports, identifying bottlenecks in the process. Possible strategies to overcome these limitations were proposed and will be investigated in future publications, especially data compression techniques and rational function based nonlinear circuit simulations.

References

[1] C. Yang, H.-D. Brüns, P. Liu, and C. Schuster, "Validation of a flexible causality treatment for transient analysis of nonlinearly loaded structures," in *2015 IEEE International Symposium on Electromagnetic Compatibility (EMC)*, 8 2015.

[2] C. Yang, P. Liu, H.-D. Brüns, and C. Schuster, "Design aspects for HIRF protection of a rectangular metallic cavity using energy selective diode grids," in *2016 Asia-Pacific International Symposium on Electromagnetic Compatibility (APEMC)*, 5 2016.

[3] S. Monni, D. J. Bekers, M. van Wanum, R. van Dijk, A. Neto, G. Gerini, and F. E. van Vliet, "Limiting frequency selective surfaces," in *2009 European Microwave Conference (EuMC)*, pp. 606–609, Sep. 2009.

[4] S. Monni, D. J. Bekers, M. van Wanum, R. van Dijk, A. Neto, G. Gerini, and F. E. van Vliet, "Protection of RF electronics using tuneable frequency selective surfaces," in *2009 3rd European Conference on Antennas and Propagation*, pp. 3170–3174, Mar. 2009.

[5] H. Wakatsuchi, D. Anzai, J. J. Rushton, F. Gao, S. Kim, and D. F. Sievenpiper, "Waveform selectivity at the same frequency," *Scientific Reports*, vol. 5, no. 1, p. 9639, 2015.

[6] G. V. Eleftheriades, "Protecting the weak from the strong," *Nature*, vol. 505, no. 7484, pp. 490–491, 2014.

[7] Z. Luo, X. Chen, J. Long, R. Quarfoth, and D. Sievenpiper, "Nonlinear power-dependent impedance surface," *IEEE Transactions on Antennas and Propagation*, vol. 63, no. 4, pp. 1736–1745, 2015.

[8] S. Kim, H. Wakatsuchi, J. J. Rushton, and D. F. Sievenpiper, "Switchable nonlinear metasurfaces for absorbing high power surface waves," *Applied Physics Letters*, vol. 108, no. 4, p. 041903, 2016.

[9] Dassault Systems, "Microwave Studio." https://www.cst.com, 2019.

[10] A. Scott and V. Sokol, "True transient 3d em/circuit co-simulation using cst studio suite," *Microwave Product Digest*, pp. 7–8, 2008.

[11] K. Aygun, B. Fischer, and J. Meng, "A fast hybrid field-circuit simulator for transient analysis of microwave circuits," *IEEE Trans. Microw. Theory Tech.*, vol. 52, no. 2, pp. 573–583, 2004.

[12] R. Wang and J. M. Jin, "Incorporation of multiport lumped networks into the hybrid time-domain finite-element analysis," *IEEE Trans. Microw. Theory Tech.*, vol. 57, no. 8, pp. 2030–2037, 2009.

[13] D. Liao, "A hybrid approach for characterizing linear and nonlinear electromagnetic scattering : Theory and applications," Tech. Rep. November, No. ARL-TR-6261. Army Research Lab, 2012.

[14] C. Yang, H.-D. Brüns, P. Liu, and C. Schuster, "Impulse response optimization of band-limited frequency data for hybrid field-circuit simulation of large-scale energy-selective diode grids," *IEEE Transactions on Electromagnetic Compatibility*, vol. 58, no. 4, pp. 1072–1080, 2016.

[15] T. Wendt, C. Yang, H. Brüns, S. Grivet-Talocia, and C. Schuster, "A macromodeling based hybrid method for the computation of transient electromagnetic fields scattered by nonlinearly loaded metal structures (submitted)." 2019.

[16] S. Silver, *Microwave antenna theory and design*, pp. 47–48. London, UK: P. Peregrinus on behalf of the Institution of Electrical Engineers, 1984.

[17] "Official website of CONCEPT-II." http://www.tet.tuhh.de/concept/, 2019.

[18] S. Grivet-Talocia and B. Gustavsen, *Passive Macromodeling*. John Wiley & Sons, Inc, 2015.

[19] S. N. Laboratories, "Xyce analog circuit simulator." https://xyce.sandia.gov, 2019.